

## Article

# Hydrogen-Rich Syngas and Biochar Production by Non-Catalytic Valorization of Date Palm Seeds

Hani Hussain Sait <sup>1,\*</sup>, Ahmed Hussain <sup>1</sup>, Mohamed Bassyouni <sup>2,3</sup> , Imtiaz Ali <sup>2</sup> , Ramesh Kanthasamy <sup>2</sup>, Bamidele Victor Ayodele <sup>4</sup> and Yasser Elhenawy <sup>5</sup> 

<sup>1</sup> Department of Mechanical Engineering, Faculty of Engineering Rabigh, King Abdulaziz University, Rabigh 21911, Saudi Arabia; ahmad@neduet.edu.pk

<sup>2</sup> Department of Chemical and Materials Engineering, Faculty of Engineering Rabigh, King Abdulaziz University, Rabigh 21911, Saudi Arabia; m.bassyouni@eng.psu.edu.eg (M.B.); inabi@kau.edu.sa (I.A.); rsampo@kau.edu.sa (R.K.)

<sup>3</sup> Department of Chemical Engineering, Faculty of Engineering, Port Said University, Port Fouad City 42526, Egypt

<sup>4</sup> Institute of Energy Policy and Research, Universiti Tenaga Nasional, Jalan Ikram-Uniten, Kajang 43000, Selangor, Malaysia; ayodele.victor@uniten.edu.my

<sup>5</sup> Department of Mechanical and Power Engineering, Faculty of Engineering, Port Said University, Port Fouad City 42526, Egypt; dr\_yasser@eng.psu.edu.eg

\* Correspondence: hhsait@kau.edu.sa

**Abstract:** Pyrolysis has been demonstrated to be a highly effective thermochemical process for converting complex biomaterials into biochar and syngas rich in hydrogen. The pyrolysis of mixed date palm seeds from Saudi Arabia was conducted using a fixed-bed pyrolyzer that was custom made for the purpose. The influence of the pyrolysis temperature (200–1000 °C) on the various physicochemical parameters of the date seed biochar generated through the pyrolysis process and the hydrogen-rich syngas was investigated. Proximate and ultimate analyses indicated a high carbon content in the lignocellulosic constituents such as cellulose, hemicellulose, and lignin. Using energy-dispersive X-ray (EDX) analysis, it was discovered that the elemental composition of biochar changes with the pyrolysis temperature. The date seeds pyrolyzed at 800 °C were found to have the maximum carbon concentration, with 97.99% of the total carbon content. The analysis of the biochar indicated a high concentration of carbon, as well as magnesium and potassium. There was a potential for the production of hydrogen-rich syngas, which increased with the pyrolysis temperature. At 1000 °C, the highest hydrogen and carbon monoxide compositions of 40 mol% and 32 mol%, respectively, were obtained. The kinetic data of the date seed pyrolysis were fitted using linearized model-free methods, such as Friedman, Flynn–Wall–Ozawa (FWO) and Kissinger–Akahira–Sunose (KAS), as well as non-linear methods such as Vyazovkin and advanced Vyazovkin. The activation energies obtained from Friedman, FWO, and KAS varied in the range of 30–75 kJ/mol, 30–65 kJ/mol, and 30–40 kJ/mol, respectively, while those of Vyazovkin and advanced Vyazovkin were found in the range of 25–30 kJ/mol, and 30–70 kJ/mol, respectively. The analysis showed that the FWO and KAS models show smaller variation compared to Friedman.

**Keywords:** biochar; biomass valorization; date palm seeds; hydrogen-rich syngas; pyrolysis; model-free kinetics



**Citation:** Sait, H.H.; Hussain, A.; Bassyouni, M.; Ali, I.; Kanthasamy, R.; Ayodele, B.V.; Elhenawy, Y. Hydrogen-Rich Syngas and Biochar Production by Non-Catalytic Valorization of Date Palm Seeds. *Energies* **2022**, *15*, 2727. <https://doi.org/10.3390/en15082727>

Academic Editor: Abdul-Ghani Olabi

Received: 19 January 2022

Accepted: 14 February 2022

Published: 8 April 2022

**Publisher's Note:** MDPI stays neutral with regard to jurisdictional claims in published maps and institutional affiliations.



**Copyright:** © 2022 by the authors. Licensee MDPI, Basel, Switzerland. This article is an open access article distributed under the terms and conditions of the Creative Commons Attribution (CC BY) license (<https://creativecommons.org/licenses/by/4.0/>).

## 1. Introduction

There is global interest in the integration of renewable energy sources to partially replace or complement conventional fossil fuels to meet future energy needs [1,2]. Biomass is a rich carbon source that can potentially be used for bioenergy or the production of high-value biochemicals through eco-friendly conversion processes [3,4]. Recent years have witnessed a paradigm shift where biomass has emerged as an essential component of

a sustainable and renewable energy network due to its renewable nature, carbon-neutral characteristics, and widespread availability [5,6]. The contribution of biomass to total renewable energy consumption for 2017 was 70% and was reported to be the third main source of electricity production after hydro and wind power [7]. In recent decades, the environmental impacts and increasing energy demand have also necessitated the use of sustainable renewable energy sources, such as wind and photovoltaic energy, in Saudi Arabia and elsewhere in the world [8]. Biomass is a valuable source of energy because it can be converted directly to biofuel, which can be used as a liquid fuel for transportation, for heat and power production, as a source of hydrogen, and can also reduce waste disposal [5,9–11]. Among the various biomass energy sources are municipal solid waste, lignocellulosic waste, industrial waste, and several organic wastes [12,13]. There are many advantages to using lignocellulosic biomass as a renewable energy source. Biomass is abundant in nature and is readily available as feedstock to produce biofuels, biomolecules, and biomaterials [14]. Furthermore, the renewable nature of biomass, its low cost, and near-zero carbon dioxide emissions are among the most significant advantages [15]. Biomass is a viable source of bioenergy due to its potential to reduce fossil fuel consumption and, thus, air pollution.

An abundant source of biomass is *Phoenix dactylifera* L., commonly known as date palm. Date palm cultivation is increasing around the world, particularly in Saudi Arabia [16,17]. Dates are the main crop of Saudi Arabia, with 1,539,756 tons produced in 2019, comprising 16.97% of worldwide production (nearly 9.1 Mtons) [18]. Saudi Arabia is the second largest producer of dates in the world after Egypt. A study has shown that the annual production of dates in Egypt, Saudi Arabia, and the rest of the world has increased exponentially in the last three decades [19]. In addition to dates being consumed raw, pitted, or stuffed with nuts, they are also increasingly used in confectionaries and baked items such as jams, jelly, puddings, biscuits, bread, and chocolates. Most uses require pitting of the dates, after which the flesh is converted to paste. During pitting, date seeds, amounting to 10–15% of the dates, are obtained as unwanted waste material, which is discarded, fed to animals, or, after removing date flesh, composted for soil amendment or burnt directly. Handling such difficult waste is problematic for manufacturing companies, who are looking for better solutions. Furthermore, from an environmental perspective, date seeds cause problems in the environment by releasing nitrogen-containing organic compounds when used as a direct fuel [20]. Some of the previous studies suggest the use of date seed oil obtained from conventional extraction techniques after catalytic upgradation [20,21].

Pyrolysis has been shown to be an effective thermochemical method for converting complex biomaterials [22–24]. It is an eco-friendly technique by which a material containing carbon can be converted into valuable gaseous, liquid, and solid products. The use of pyrolysis for biomass valorization has been widely reported in the literature [25–27]. Santos et al. [28] investigated the kinetics and thermodynamic parameters of pyrolyzed Acai seed biomass using thermogravimetric analysis. Activation energies of 159.12 kJ/mol and 157.62 kJ/mol were obtained using the FWO and KAS model-free equations, respectively. Zheng et al. [29] investigated the pyrolysis and catalytic co-pyrolysis upgrading of biomass and waste rubber seed oil to stimulate the formation of aromatic hydrocarbons. The study revealed that the yields of benzene, toluene, xylene, and ethylbenzene were up to 78.77% from the pyrolysis process. Mishra et al. [30] investigated the catalytic pyrolysis of pine sawdust and Gulmohar seed for the production of fuel and chemicals. The total pyrolytic liquid yield obtained from pyrolysis was found to be 39.39% and 36.68% for pine sawdust and Gulmohar seed, respectively. Mishra et al. [31] also reported the pyrolysis kinetic behavior of *Samanea saman* seeds towards the production of renewable fuel. The pyrolysis resulted in a pyrolytic liquid of 44.20 wt%. In this study, date seeds were pyrolyzed thermochemically in a customized fixed-bed pyrolyzer to produce hydrogen-rich syngas and biochar that have a wide range of applications in industry [32].

## 2. Materials and Methods

### 2.1. Preparation and Characterization of Date Seeds

The local date seeds were washed and dried in air for 2 days. Air-dried seeds were ground in a 1500 W multifunctional high-speed grinder. The undersize powder sieved through 200 mesh with particles up to 500 microns was kept for further analysis. Biomass samples were proximately analyzed using ASTM D3173 (moisture), ASTM D3174 (ash), and ASTM D3175 (volatile materials) techniques. The ultimate analysis of the sample was determined using an elemental analyzer. A scanning electron microscope (Schottkyfield emission, JSM-7610F) coupled with energy-dispersive X-ray spectroscopy was used to examine biochar morphology and elemental composition at a 5 kV accelerating voltage. The heating values of the samples were determined using an ASTM D5865-13 standard procedure and a CAL-2 K Oxygen Bomb Calorimeter. The gaseous product compositions were analyzed using GC-TCD-FID. Both Supelco Molecular Sieve 13 $\times$  (10 feet 1/8 inch diameter, 2 mm ID, 60/80 mesh, stainless steel) and Agilent Hayesep DB (30 feet 1/8 inch diameter, 2 mm ID, 100/120 mesh, stainless steel) packed columns were employed in this study. With an operating column temperature of 120 °C and detector temperature of 150 °C (column pressure of 90 psi), helium gas was utilized as a carrier at a flow rate of 20 mL/min. A Hayesep DB column was used for the separation and quantification of gas analytes such as H<sub>2</sub>, CH<sub>4</sub>, and C<sub>2</sub>H<sub>6</sub>. A Molecular Sieve 13 $\times$  column was used for the separation and quantification of CO.

### 2.2. Fixed-Bed Pyrolyzer Setup

A custom-made fixed bed pyrolyzer, as shown in Figure 1, was used for this study. The setup consists of a vertical tubular reactor made up of inox steel with an inner diameter of 15 cm and a height of 30 cm. Electrical heating coils surround the reactor with thick fiberboard insulation provided inside the assembly. The sample holder is placed in the heating region inside the reactor on a support connected to a thin rod passing through a bottom hole. The other side of the rod comes into direct contact with a digital scale that is connected to a programmable logic controller (PLC). Mass of the sample is displayed in real time on the display screen of the control panel, along with the time and temperature at the same time recorded by the data logger. A constant flow of pure nitrogen gas at 500 mL/min is swept through the furnace to displace air from the system for 30 min before starting the experiment. This step ensures that no air remains in the furnace and an inert environment is achieved. A continuous and constant flow of nitrogen gas is maintained with the help of a digital flow meter connected to the PLC, while the heating step is controlled by the heating power of the furnace and the response of the thermocouple. Around 50 g of the dry powder was loaded onto the sample holder for each measurement. The furnace was preheated at 105 °C for 30 min to remove excess moisture. Subsequently, the temperature was gradually increased to 1000 °C/min. During the experiment, the mass, temperature, and time were recorded.

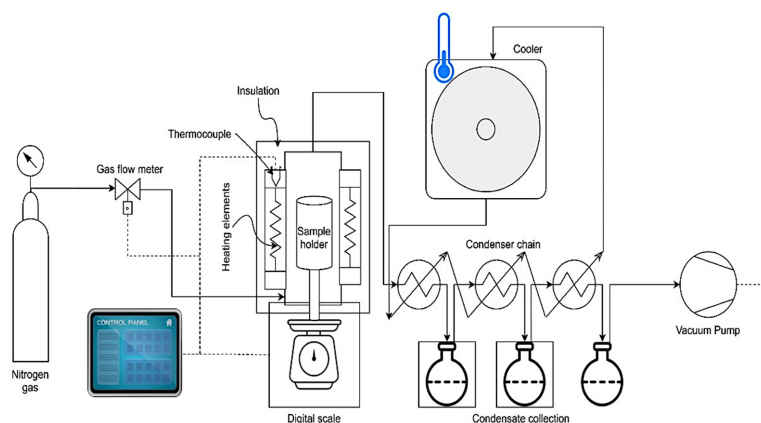


**Figure 1.** Schematic representation of the custom-made fixed-bed fast pyrolyzer.

### 2.3. Kinetics of Pyrolysis

Thermal conversion is based on the differential rate expression shown in Equation (1), which numerically describes the rate of a reaction ( $\frac{d\alpha}{dt}$ ) proportional to the reaction model  $f(\alpha)$ . The proportionality constant is termed as the rate constant  $k(T)$ .

$$\frac{d\alpha}{dt} = k(T)f(\alpha) \quad (1)$$

From Arrhenius, the rate constant is the product of the pre-exponential coefficient  $A$  and the exponential of  $-\frac{E_a}{RT}$  where  $E_a$  is an important term called the activation energy or the energy barrier in the conversion of reactants to products measured in  $\text{kJ mol}^{-1}$ . The expanded form of the differential rate expression can thus be written as shown in Equation (2).

$$\frac{d\alpha}{dt} = A \exp\left(-\frac{E_a}{RT}\right)f(\alpha) \quad (2)$$

Equation (2) can be linearized, resulting in Equation (3), which was used by Friedman to perform the kinetic analysis.

$$\ln\left(\frac{d\alpha}{dt}\right) = \ln[A \cdot f(\alpha)] - \frac{E_a}{RT} \quad (3)$$

However, the derivative of conversion with respect to time makes this equation sensitive to noise. The integral solution of Equation (3) is not straightforward, and the alternative analytical solutions somehow contain inaccuracies. The most frequent integral equations are Flynn–Wall–Ozawa (FWO) and Kissinger–Akahira–Sunose (KAS). Since the linear equations are independent of  $f(\alpha)$ , they are referred to as model-free methods (Equations (4) and (5)).

$$\text{FWO} \quad \ln \beta = \text{const} - 1.052 \frac{E_a}{RT} \quad (4)$$

$$\text{KAS} \quad \ln\left(\frac{\beta}{T^2}\right) = \text{const} - \frac{E_a}{RT} \quad (5)$$

Vyazovkin and advanced Vyazovkin methods are non-linear integral methods (Equations (6) and (7)). The advanced Vyazovkin method is considered to be more accurate and matches the Friedman calculation well. For a set of  $n$  trials carried out at different heating programmes,  $T_i(t)$ , the activation energy, may be estimated for any given value of conversion using the Vyazovkin technique by identifying the value of  $E_a$  that minimizes the following functions:

$$\text{Vyazovkin: } \Phi(E_a) = \min \sum_i^N \sum_{i \neq j}^N \left[ \frac{I(E_a, T_{ai}) \cdot \beta_j}{I(E_a, T_{aj}) \cdot \beta_i} \right] \quad (6)$$

$$\text{Advanced Vyazovkin: } \Phi(E_a) = \min \sum_{i=1}^N \sum_{i \neq j}^N \frac{J[E_a, T_i(E_a)]}{J[E_a, T_j(E_a)]} \quad (7)$$

Subscripts  $i$  and  $j$  denote the number of different heating rates that were utilized to investigate the pyrolysis process. The integral is calculated numerically as shown in Equation (8):

$$J[E_a, T_i(t_\alpha)] = \int_{t_{\alpha-\Delta\alpha}}^{t_\alpha} \exp\left(\frac{-E_a}{RT_i(t)}\right) dt \quad (8)$$

From Equation (8),  $\Delta\alpha$  is the conversion increment, which is commonly set to 0.01, which is adequate to minimize accumulation of the errors in the calculation of  $E_a$ ,  $t$  is the time, and  $J$  is the temperature integral, which can be numerically assessed using the trapezoidal rule.

### 3. Results and Discussion

#### 3.1. Characterization of Date Seeds

The physicochemical and thermal properties of the date seeds obtained from the proximate analysis and the ultimate analysis, the determination of the lignocellulosic content, and the thermal analysis are summarized in Table 1. The proximate analysis shows that the date seeds consist of 4.1% moisture, 78% volatile matter, 9.2% fixed carbon, and 8.25% ash. The values obtained for the proximate analysis of the date seed are consistent with those reported in the literature. The proximate analysis of biomass helps to determine the percentage of material that burns as volatile matter, as fixed carbon, and the amount of ash. This information is critical for the use of biomass energy. Fixed carbon from biomass has a positive correlation with charcoal production, but volatile carbon and ash have a negative correlation [28]. As a result, it is reasonable to assume that increasing the volatile components of biomass will lead to higher production of the gas phase rather than the solid phase. The ultimate analysis shows that the date seed contains 47.15% carbon, 7.52% hydrogen, 0.82% nitrogen, 44% oxygen, which is typical of lignocellulosic biomass. The ultimate analysis is evidence of the suitability of the date seed as a feedstock that can be used for the production of renewable energy. Date seed, a lignocellulosic biomass, consists of 33.1% cellulose, 24.3% hemicellulose, and 22.6% lignin. The distribution of the different elements in various lignocellulosic constituents is in the range of literature reports. This implies that date seeds are a good source of bioenergy and can also be used to obtain a wide range of bioproducts. The HHV value of 18.7 MJ/kg obtained for date seeds is an indication of good-quality fuel.

**Table 1.** Physicochemical and thermal properties of date seeds.

		This Study	[8]	[9]	[11]	[12]
Proximate (wt%)	Moisture	4.1	4–4.5			
	Volatile matter	78.5	78–80.1	83.33		
	Fixed carbon	9.2	5.4–9.9	14.94		
	Ash	8.2	7.7–11.5	1.4		
Ultimate (wt%)	C	47.15		47.14		
	H	7.52		6.63		
	N	0.82		0.9		
	O	44.51		45.3		
Lignocellulose (wt%)	Cellulose	33.1		33.77	26.6–33.92	23.9
	Hemicellulose	24.3		30.20	31.97–42.3	26.8
	Lignin	22.6		37.03	21.2–24.06	216
Thermal (MJ/kg)	HHV	18.7	18.226–18.548			

The elemental composition of the date seed based on the EDX analysis as a function of the valorization temperature is summarized in Table 2. Evidence of the various elemental compositions obtained from the EDX analysis is shown in Figure 2. The intensity of each elemental composition in the micrograph depicts the amount of each element in the valorized date seed. Basically, the valorized date seed consists of carbon, oxygen, magnesium, and phosphorus in varying proportions, depending on the temperature. At 400 °C, the valorized date seeds mainly contain carbon (88%), followed by 10.28% oxygen, 0.28% magnesium, and 0.48% phosphorus. At 500 °C, the carbon content of the valorized date seeds increased to 94.6%, while the oxygen, magnesium, and phosphorus contents decreased to 4.66%, 0.13%, and 0.21%, respectively. A trace sulfur content of 0.31% was also observed. A further increase in temperature to 800 °C resulted in an increase in carbon content to 97.99%, with some traces of oxygen, magnesium, and phosphorus. However, there was a sharp decrease in the carbon content at a valorization temperature of 1000 °C. This can be attributed to the presence of other components present in the valorized date seed at 1000 °C. The high carbon content in the valorized seed date makes it a possible source of adsorbent materials that can be used for wastewater treatment. Sayed et al. [33] used a low-cost adsorbent prepared from date seed for the removal of thorium ions from solutions of acidic media. A high adsorption capacity of 43 mg/g was reported for the date seed-based adsorbent. In addition, Haddabi et al. [34] reported the use of date seed ash to

remove boron from seawater. The use of the date seed-based adsorbent resulted in 47% removal efficiency of boron from seawater.

**Table 2.** Elemental composition of date palm seeds valorized at different temperatures.

Element	Atomic Weight (%) at 400 °C	Atomic Weight (%) at 600 °C	Atomic Weight (%) at 800 °C	Atomic Weight (%) at 1000 °C
Carbon (C)	88.96 ± 0.21	94.69 ± 0.20	97.99 ± 0.14	93.88 ± 0.16
Oxygen (O)	10.28 ± 0.11	4.66 ± 0.10	0.70 ± 0.20	4.75 ± 0.14
Magnesium (Mg)	0.28 ± 0.02	0.13 ± 0.03	0.32 ± 0.02	0.52 ± 0.10
Phosphorus (P)		0.21 ± 0.02	0.99 ± 0.11	0.24 ± 0.03
Sulfur (S)			0.14 ± 0.01	0.13 ± 0.01
Potassium (K)	0.48 ± 0.01	0.31 ± 0.10		0.40 ± 0.01
Calcium (Ca)				0.08 ± 0.12

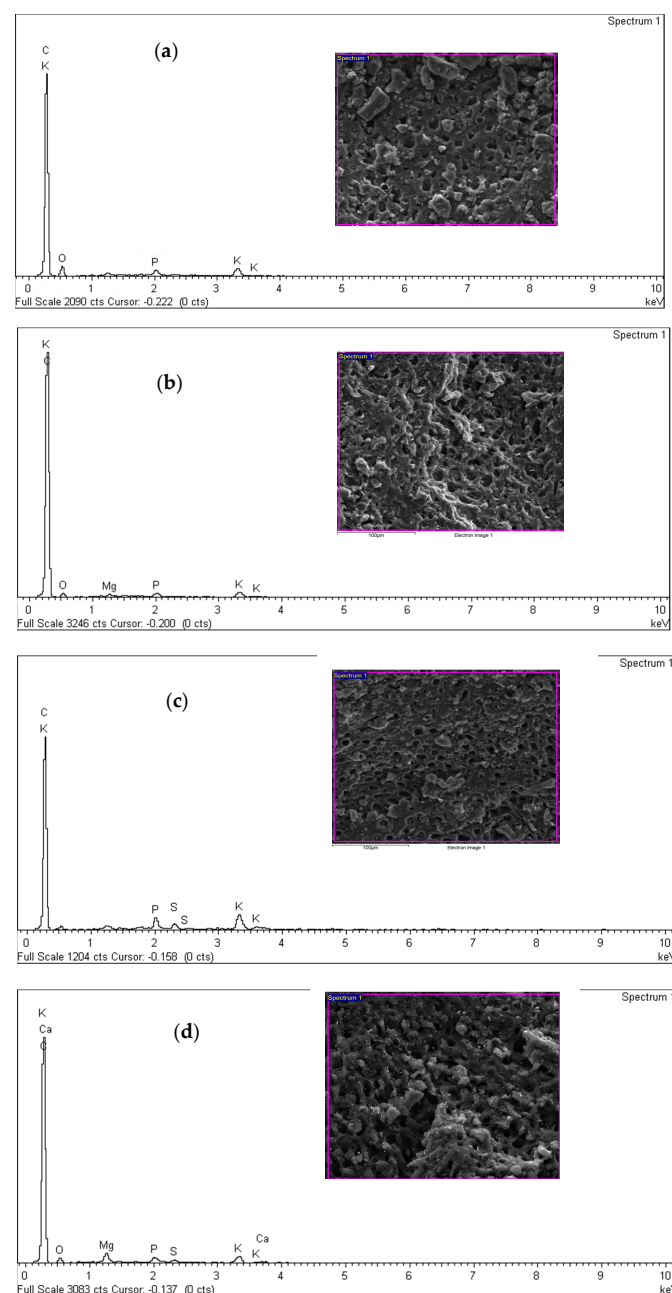


**Figure 2.** EDX micrograph of the valorized date seed at (a) 400 °C (b) 600 °C (c) 800 °C, and (d) 1000 °C.

The SEM images showing the valorized date seed at different temperatures are depicted in Figure 3a–d. It can be seen that there is evidence of a high carbon content with varying micropores. The micropores increase with increases in the vaporization temperature from 400 to 1000 °C. The comparison of the SEM images revealed that impurities could be identified at a lower valorization temperature of 400 to 600 °C (Figure 3a,b). A clearer image, presented in Figure 3c,d, should be a purer valorized date seed with high-quality carbon. Mahdi et al. [35] reported that modified biochar obtained from valorized date seeds at temperatures of >500 °C develops more micropores due to the removal of impurities.

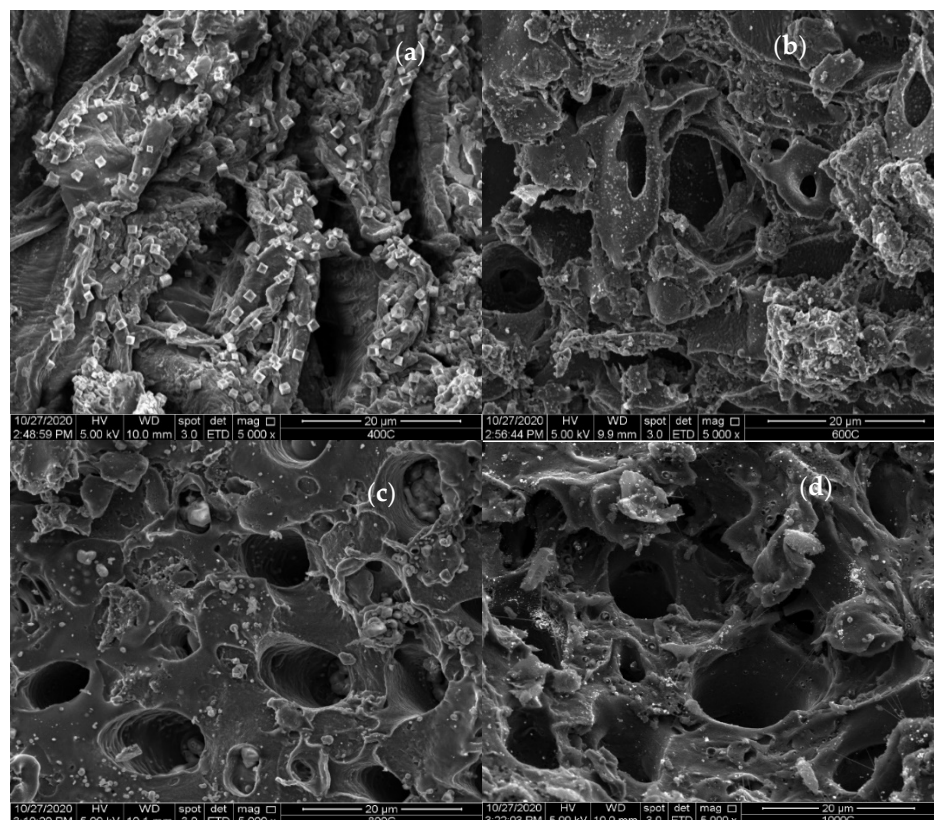


**Figure 3.** SEM images of the valorized date seed at (a) 400 °C, (b) 600 °C, (c) 800 °C, and (d) 1000 °C.

### 3.2. Fast Pyrolysis Temperature and Heating Rate

The temperature profiles showing the conversion and weight loss of the date seed during pyrolysis are shown in Figure 4. The effect of four different heating rates (2.5, 5, 7.5, and 10 °C/min) on conversion and weight loss was examined. The shape of the conversion rate profiles in Figure 4 is indicative of complex degradation in the active pyrolysis zone. This shape clearly shows the convolution of different peaks, which indicates that the constituents are simultaneously undergoing degradation. Like other lignocellulosic materials, date seed pyrolysis also consisted of convoluted degradations of hemicellulose, cellulose, and lignin. Different peaks centered at 450 °C, 550 °C, 620 °C, and 720 °C can be attributed to conversion of the different constituents of the date seed. The conversion process could result in the formation of various products. In this study, the focus is on biochar conversion. The left shoulder of the main peak corresponds to hemicellulose pyrolysis, the right shoulder corresponds to cellulose pyrolysis, and the convulsing shoulder corresponds to the delayed degradation of lignin. Zhou et al. [13] reported the pyrolysis of hemicellulose, cellulose, and lignin at 10 °C/min. The authors revealed that hemicellulose degrades between 220–315 °C, while cellulose conversion occurs in a narrower temperature range of 315–400 °C. The conversion of lignin often occurs in a wider temperature range, from 160 to 900 °C. The authors reported that 40% of the solid residue was the result of lignin

pyrolysis. For a fixed-bed reactor, the delay in conversion can be attributed to thermal lag. According to Khiari and Jeguirim [36], cellulose and hemicellulose degradation occurs between 166 and 362 °C. The decomposition of lignin occurs between 362 °C and 500 °C. The final stage of lignin degradation occurs in passive pyrolysis and char production and rearrangement, which is marked by a modest and constant mass loss rate. After the release of oxygen and vapors from the product, a variety of reactions occur, including cracking, reforming, dehydration, condensation, polymerization, and even oxidation and gasification reactions. The effects of the fast pyrolysis temperature on the gaseous distribution of date seed pyrolysis are depicted in Figure 5. It can be seen that an increase in the pyrolysis temperature significantly influences the product distribution. Syngas ( $H_2$  and  $CO$ ) can be seen to increase with an increase in pyrolysis temperature, resulting in the highest composition of  $H_2$  and  $CO$  of 40 mol% and 32 mol%, respectively. However,  $CH_4$  and  $C_2H_6$  were observed to decrease with increasing pyrolysis temperature. The  $CO_2$  composition (not shown in Figure 5) increases from 0.9 mol.% at 200 °C to 5.6 mol.% at 1000 °C. This can be attributed to the increasing breakage of the C-H bond in the date seed as the temperature increases.

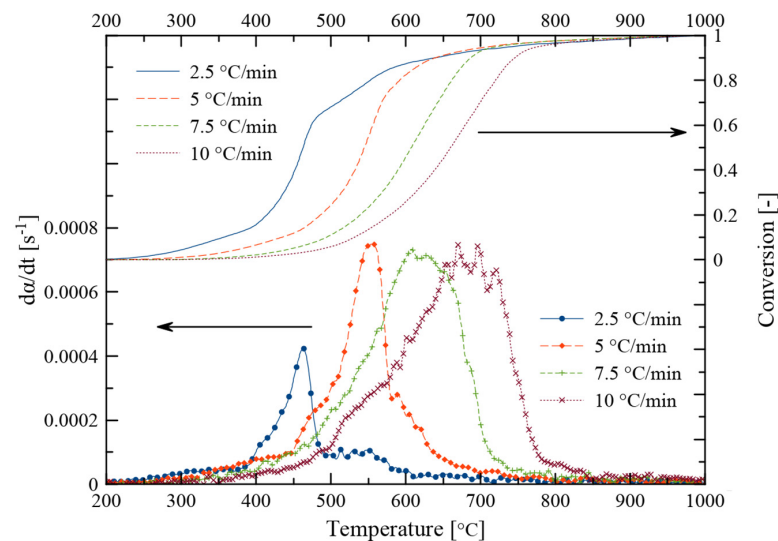


**Figure 4.** Conversion and conversion rate curves for date seed pyrolysis.

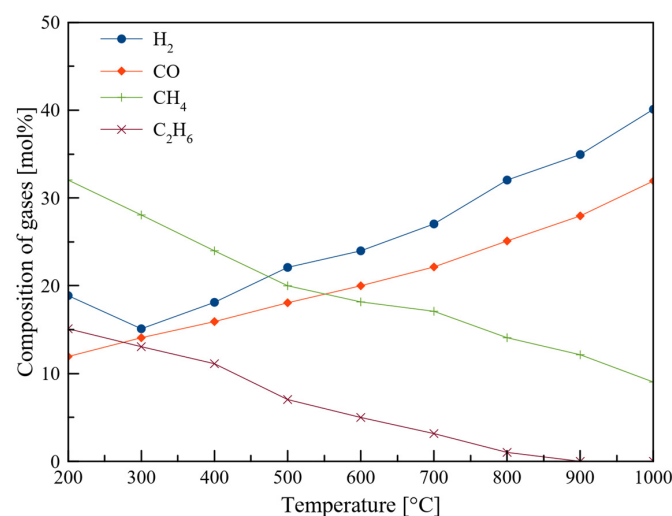


**Figure 5.** Effect of temperature on the composition of gaseous products from fast pyrolysis of date palm at heating rate of 100 °C/min.

### 3.3. Kinetic Analysis

Figure 6 shows the linear plots of the Friedman, Flynn–Wall–Ozawa (FWO), and Kissinger–Akahira–Sunose (KAS) models. The Friedman, FWO, and KAS activation energies vary in the range of 30–75 kJ/mol, 30–65 kJ/mol, and 30–40 kJ/mol, respectively. As the conversion rates increase, the activation energy decreases. Low activation energy values are believed to be necessary for the good thermal decomposition of biomass. Several cellulosic biomasses showed a steady decrease in the apparent activation energy. On the basis of the kinetics of the decomposition, amorphous cellulose and hemicellulose are quickly and easily broken apart by the rapid and first scission of the loosely linked fibers. Lignin contributed to a further drop in activation energy after the decomposition of all-crystalline cellulose. Khiari and Jeguirim [36] reported the application of the Friedman, FWO, and KAS models in describing the pyrolysis of grape marc from Tunisia. The apparent activation energies of 229.5, 226.8, and 224.2 kJ/mol were obtained using the Friedman, FWO, and KAS models, respectively. The authors reiterate the importance of the kinetics data as crucial in the design of the pyrolyzer for the recovery of Tunisian grape marc. Furthermore, Ondro et al. [36] also employed the Friedman, FWO, and KAS models to test the kinetic data obtained from air pyrolysis of spruce wood in a temperature range of 260–360 °C. Kinetic analysis resulted in apparent activation energies in the range of 168.6–196.5 kJ/mol, 179.8–188.1 kJ/mol, and 170.1–178.7 kJ/mol for Friedman, FWO, and KSA, respectively. In a similar study, Gao et al. [37] applied Friedman and KSA. The activation energies of 244.25 and 238.07 kJ/mol of the date palm pyrolysis reaction were obtained using Friedman and KAS models, respectively. Variations in the activation energies of the various biomasses could be attributed to their lignocellulosic compositions.

Kinetic data sets with heating rates of 2.5, 5, 7.5, and 10 °C/min were analyzed using isoconversional methods. As shown in Figure 7, the apparent activation energies ( $E_a$ ) of each of the models vary with the conversion of the pyrolyzed date seed. The  $E_a$  calculated from the FWO and KAS methods is further from that of the Friedman method. The Vyazovkin and advanced Vyazovkin methods are non-linear methods. The  $E_a$  values obtained from the Vyazovkin model are relatively consistent with the KAS, whereas the advanced Vyazovkin  $E_a$  estimations are close to that of Friedman. However, the  $E_a$  values obtained from both Vyazovkin and Friedman vary significantly. Further, it can be seen that at a 0.6 conversion level, an increase in  $E_a$  can be observed, which is significant in the Friedman and advanced Vyazovkin methods. Different macro-component decompositions are responsible for the varying  $E_a$  values at various conversion stages. The  $E_a$  of 25 to 100 kJ/mol can be attributed to hemicellulose breakdown at low conversion levels (0.2 to 0.4). The decrease in  $E_a$  in the range of 40–60 kJ/mol can be attributed to cellulose breakdown at conversion levels of 0.45 and 0.80. It is assumed that lignin is responsible for increasing the activation energy of the KAS and OFW models, as well as the Friedman model, at higher conversion levels. Studies have shown that activation energies drop with increasing temperature, which can be explained by the continued decomposition of cellulose and lignin, as well as the rearrangement of biochar through secondary and more complex processes. The  $R^2$  values obtained for each of the models at different conversions are summarized in Table 3. Higher  $R^2$  and lower standard deviation values are obtained from fittings of the KAS and FWO models. Hence, it can be adjudged that the KAS and FWO models provide activation energies with lower variation compared to that obtained from Friedman method with lower  $R^2$  [38–40].

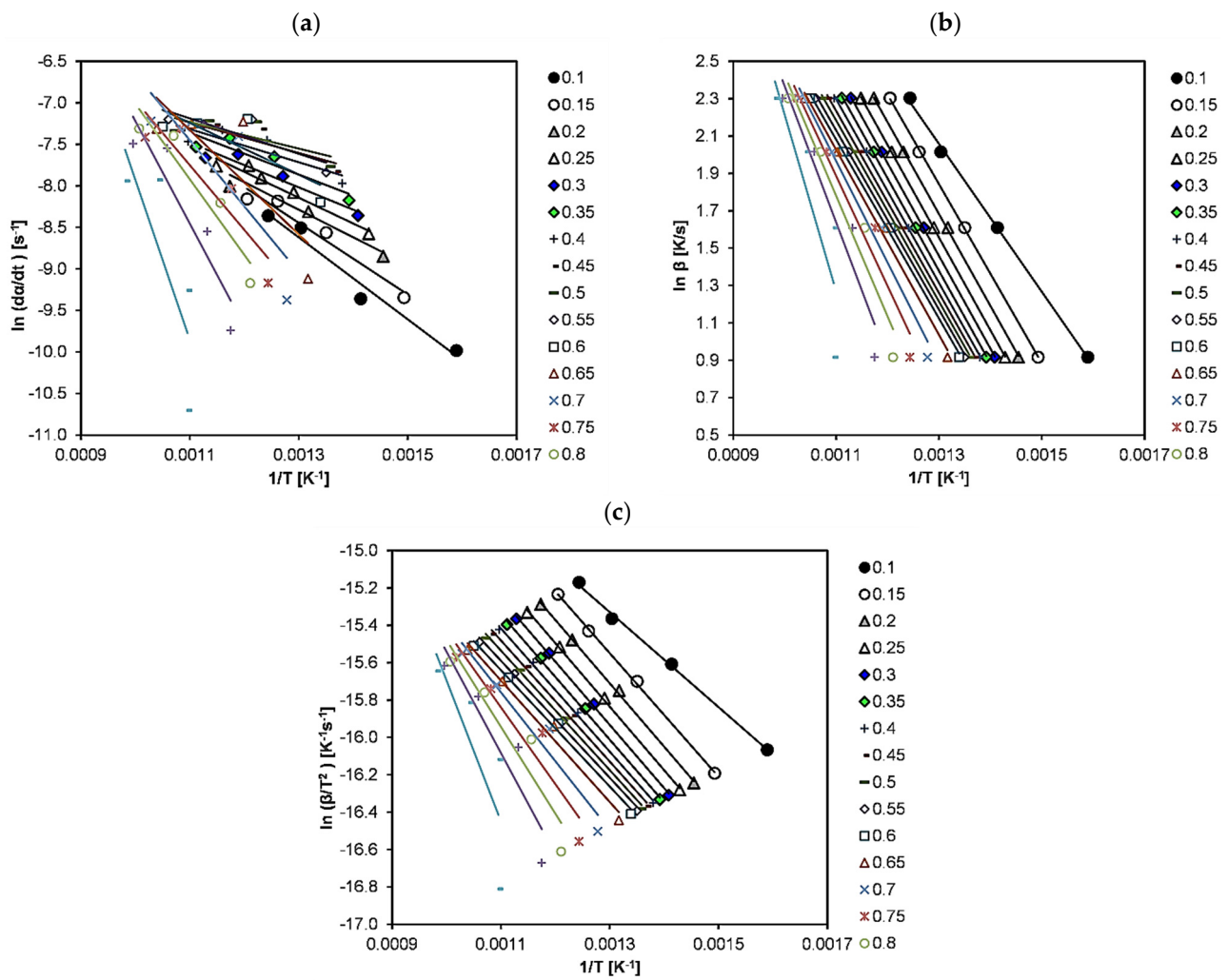


Figure 6. Linear regression of (a) Friedman, (b) FWO, and (c) KAS equations at different conversions.

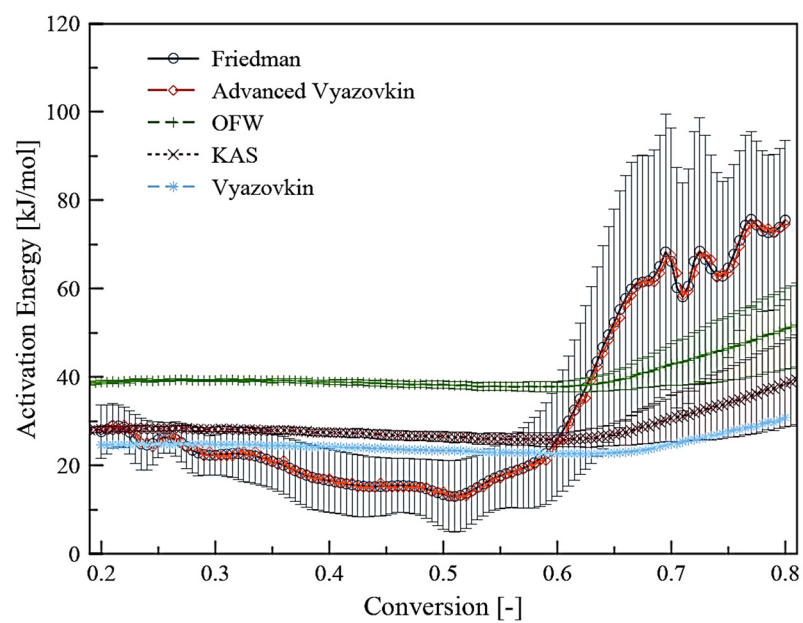


Figure 7. Activation energy as a function of conversion for the linear and non-linear methods.

**Table 3.** Summary of  $E_a$  and  $R^2$  obtained from the fittings of each model.

$\alpha$	Vyazovkin	Advanced Vyazovkin	Friedman		KAS		FWO	
	$E_a$ (kJ/mol)	$E_a$ (kJ/mol)	$E_a$ (kJ/mol)	$R^2$	$E_a$ (kJ/mol)	$R^2$	$E_a$ (kJ/mol)	$R^2$
0.20	24.66	29.19	27.62	0.91	28.19	1.00	38.85	1.00
0.25	24.85	25.15	25.85	0.95	28.29	1.00	39.18	1.00
0.30	24.67	22.12	22.34	0.92	28.15	1.00	39.24	1.00
0.35	24.50	21.11	20.95	0.85	27.90	1.00	39.17	1.00
0.40	24.18	16.06	16.53	0.73	27.44	1.00	38.87	1.00
0.45	23.78	15.05	15.24	0.73	26.94	1.00	38.53	1.00
0.50	23.40	16.06	13.40	0.60	26.57	1.00	38.30	1.00
0.55	22.92	16.06	17.69	0.74	26.01	0.99	37.87	1.00
0.60	22.69	24.14	25.91	0.67	25.85	0.99	37.84	1.00
0.65	22.88	50.40	52.39	0.68	27.03	0.98	39.16	0.99
0.70	24.89	66.56	66.08	0.71	30.66	0.94	42.90	0.98
0.75	27.56	63.53	64.72	0.84	34.13	0.91	46.48	0.95
0.80	30.83	74.64	75.49	0.90	38.56	0.88	50.97	0.94

#### 4. Conclusions

This study has investigated the pyrolysis of date palm seeds in a fixed-bed pyrolyzer at varying heating rates of 2.5, 5, 7.5, and 10 °C/min to produce biochar. The final analysis of the date seed powder shows that carbon, hydrogen, and oxygen were present primarily in the lignocellulosic structure, which consisted of 33.1 wt% cellulose, 24.3 wt% hemicellulose and 22.6 wt% lignin. The conversion rate profiles indicated that the complex degradation of the date seed during pyrolysis occurs in the active pyrolysis zone. Kinetic analyses were performed using linear regression of model-free methods, such as Friedman, FWO, and KAS, as well as Vyazovkin and advanced Vyazovkin non-linear methods. FWO and KAS show less variation than Friedman. A similar trend can also be seen in the activation energy profile. The Friedman, FWO, and KAS activation energies vary in the ranges of 30–75 kJ mol<sup>-1</sup>, 30–65 kJ mol<sup>-1</sup>, and 30–40 kJ/mol, respectively. Those of Vyazovkin and advanced Vyazovkin are in the range of 25–30 kJ mol<sup>-1</sup> and 30–70 kJ/mol, respectively. Fitting the KAS and FWO models with the data resulted in higher  $R^2$  and lower standard deviation values than those obtained from other models. As a result, it can be concluded that the KAS and FWO models produce activation energies with smaller fluctuations when compared to those derived using the Friedman technique, which has a lower  $R^2$  value. These kinetic parameters may help facilitate the design of a suitable pyrolyzer for date seed obtained from Saudi Arabia.

**Author Contributions:** Conceptualization, H.H.S.; methodology, H.H.S. and A.H.; software, H.H.S. and M.B.; validation, I.A. and R.K.; formal analysis, I.A. and R.K.; investigation, M.B. and R.K.; resources, H.H.S.; data curation, B.V.A.; writing—H.H.S. and R.K.; writing—review and editing, H.H.S., I.A. and B.V.A.; visualization, M.B.; supervision, H.H.S.; project administration, H.H.S.; funding acquisition, H.H.S. and Y.E.; writing—review and editing. All authors have read and agreed to the published version of the manuscript.

**Funding:** This research was funded by the National plan for Science, Technology, and Innovation MAARIFAH—King Abdulaziz City for Science and Technology—The Kingdom of Saudi Arabia—Award No. 11-WAT2033-03. The authors also acknowledge with thanks the staff at the Science and Technology Unit of King Abdulaziz University in Jeddah for their technical support.

**Data Availability Statement:** No new data were created or analyzed in this study. Data sharing is not applicable to this article.

**Conflicts of Interest:** The authors declare no conflict of interest.

## References

1. Sgouridis, S.; Griffiths, S.; Kennedy, S.; Khalid, A.; Zurita, N. A sustainable energy transition strategy for the United Arab Emirates: Evaluation of options using an Integrated Energy Model. *Energy Strategy Rev.* **2013**, *2*, 8–18. [[CrossRef](#)]
2. Ray, P. Renewable energy and sustainability. *Clean Technol. Environ. Policy* **2019**, *21*, 1517–1533. [[CrossRef](#)]
3. Raud, M.; Kikas, T.; Sippula, O.; Shurpali, N.J. Potentials and challenges in lignocellulosic biofuel production technology. *Renew. Sustain. Energy Rev.* **2019**, *111*, 44–56. [[CrossRef](#)]
4. Habibollahzade, A.; Ahmadi, P.; Rosen, M.A. Biomass gasification using various gasification agents: Optimum feedstock selection, detailed numerical analyses and tri-objective grey wolf optimization. *J. Clean. Prod.* **2021**, *284*, 124718. [[CrossRef](#)]
5. Zheng, Y.; Jenkins, B.M.; Kornbluth, K.; Kendall, A.; Træholt, C. Optimization of a biomass-integrated renewable energy microgrid with demand side management under uncertainty. *Appl. Energy* **2018**, *230*, 836–844. [[CrossRef](#)]
6. Perea-Moreno, M.-A.; Samerón-Manzano, E.; Perea-Moreno, A.-J. Biomass as Renewable Energy: Worldwide Research Trends. *Sustainability* **2019**, *11*, 863. [[CrossRef](#)]
7. Gielen, D.; Boshell, F.; Saygin, D.; Bazilian, M.D.; Wagner, N.; Gorini, R. The role of renewable energy in the global energy transformation. *Energy Strategy Rev.* **2019**, *24*, 38–50. [[CrossRef](#)]
8. Amran, Y.H.A.; Amran, Y.H.M.; Alyousef, R.; Alabduljabbar, H. Renewable and sustainable energy production in Saudi Arabia according to Saudi Vision 2030; Current status and future prospects. *J. Clean. Prod.* **2020**, *247*, 119602. [[CrossRef](#)]
9. Niphadkar, S.; Bagade, P.; Ahmed, S. Bioethanol production: Insight into past, present and future perspectives. *Biofuels* **2018**, *9*, 229–238. [[CrossRef](#)]
10. Hannula, I. Hydrogen enhancement potential of synthetic biofuels manufacture in the European context: A techno-economic assessment. *Energy* **2016**, *104*, 199–212. [[CrossRef](#)]
11. Silva, V.; Rouboas, A. Optimizing the gasification operating conditions of forest residues by coupling a two-stage equilibrium model with a response surface methodology. *Fuel Process. Technol.* **2014**, *122*, 163–169. [[CrossRef](#)]
12. Salam, M.A.; Ahmed, K.; Akter, N.; Hossain, T.; Abdullah, B. A review of hydrogen production via biomass gasification and its prospect in Bangladesh. *Int. J. Hydrogen Energy* **2018**, *43*, 14944–14973. [[CrossRef](#)]
13. Zhou, H.; Long, Y.; Meng, A.; Chen, S.; Li, Q.; Zhang, Y. A novel method for kinetics analysis of pyrolysis of hemicellulose, cellulose, and lignin in TGA and macro-TGA. *RSC Adv.* **2015**, *5*, 26509–26516. [[CrossRef](#)]
14. Kim, J.Y.; Lee, H.W.; Lee, S.M.; Jae, J.; Park, Y.K. Overview of the recent advances in lignocellulose liquefaction for producing biofuels, bio-based materials and chemicals. *Bioresour. Technol.* **2019**, *279*, 373–384. [[CrossRef](#)] [[PubMed](#)]
15. Ayodele, B.V.; Mustapa, S.I.; Tuan Abdullah, T.A.R.; Bin Salleh, S.F. A Mini-Review on Hydrogen-Rich Syngas Production by Thermo-Catalytic and Bioconversion of Biomass and Its Environmental Implications. *Front. Energy Res.* **2019**, *7*, 118. [[CrossRef](#)]
16. Sait, H.H.; Hussain, A.; Salema, A.A.; Ani, F.N. Pyrolysis and combustion kinetics of date palm biomass using thermogravimetric analysis. *Bioresour. Technol.* **2012**, *118*, 382–389. [[CrossRef](#)] [[PubMed](#)]
17. Salama, K.F.; Randhawa, M.A.; Mulla, A.A.; Al Labib, O.A. Heavy metals in some date palm fruit cultivars in Saudi Arabia and their health risk assessment. *Int. J. Food Prop.* **2019**, *22*, 1684–1692. [[CrossRef](#)]
18. Hussain, A.; Farooq, A.; Bassyouni, M.I.; Sait, H.H.; El-Wafa, M.A.; Hasan, S.W.; Ani, F.N. Pyrolysis Of Saudi Arabian Date Palm Waste: A Viable Option For Converting Waste Into Wealth. *Life Sci. J.* **2014**, *11*, 667–671.
19. Mujica, R. *10 World's Biggest Countries in Date Production of 2019*; Azhan Co.: Shah Alam, Malaysia, 2020.
20. Rambabu, K.; Show, P.-L.; Bharath, G.; Banat, F.; Naushad, M.; Chang, J.-S. Enhanced biohydrogen production from date seeds by *Clostridium thermocellum* ATCC 27405. *Int. J. Hydrogen Energy* **2020**, *45*, 22271–22280. [[CrossRef](#)]
21. Mrabet, A.; Jiménez-Araujo, A.; Guillén-Bejarano, R.; Rodríguez-Arcos, R.; Sindic, M. Date Seeds: A Promising Source of Oil with Functional Properties. *Foods* **2020**, *9*, 787. [[CrossRef](#)]
22. Kabir, G.; Mohd Din, A.T.; Hameed, B.H. Pyrolysis of oil palm mesocarp fiber catalyzed with steel slag-derived zeolite for bio-oil production. *Bioresour. Technol.* **2018**, *249*, 42–48. [[CrossRef](#)] [[PubMed](#)]
23. Mohan, D.; Pittman, C.U., Jr.; Steele, P.H. Pyrolysis of Wood/Biomass for Bio-oil: A Critical Review. *Energy Fuels* **2006**, *20*, 848–889. [[CrossRef](#)]
24. Gallezot, P. Conversion of biomass to selected chemical products. *Chem. Soc. Rev.* **2012**, *41*, 1538–1558. [[CrossRef](#)] [[PubMed](#)]
25. Hameed, S.; Sharma, A.; Pareek, V.; Wu, H.; Yu, Y. A review on biomass pyrolysis models: Kinetic, network and mechanistic models. *Biomass Bioenergy* **2019**, *123*, 104–122. [[CrossRef](#)]
26. Hu, X.; Gholizadeh, M. Biomass pyrolysis: A review of the process development and challenges from initial researches up to the commercialisation stage. *J. Energy Chem.* **2019**, *39*, 109–143. [[CrossRef](#)]
27. Wang, S.; Dai, G.; Yang, H.; Luo, Z. Lignocellulosic biomass pyrolysis mechanism: A state-of-the-art review. *Prog. Energy Combust. Sci.* **2017**, *62*, 33–86. [[CrossRef](#)]
28. Santos, V.O.; Queiroz, L.S.; Araujo, R.O.; Ribeiro, F.C.P.; Guimarães, M.N.; da Costa, C.E.F.; Chaar, J.S.; de Souza, L.K.C. Pyrolysis of acai seed biomass: Kinetics and thermodynamic parameters using thermogravimetric analysis. *Bioresour. Technol. Rep.* **2020**, *12*, 100553. [[CrossRef](#)]

29. Zheng, Y.; Tao, L.; Yang, X.; Huang, Y.; Liu, C.; Zheng, Z. Insights into pyrolysis and catalytic co-pyrolysis upgrading of biomass and waste rubber seed oil to promote the formation of aromatics hydrocarbon. *Int. J. Hydrogen Energy* **2018**, *43*, 16479–16496. [[CrossRef](#)]
30. Mishra, R.K.; Mohanty, K. Thermal and catalytic pyrolysis of pine sawdust (*Pinus ponderosa*) and Gulmohar seed (*Delonix regia*) towards production of fuel and chemicals. *Mater. Sci. Energy Technol.* **2019**, *2*, 139–149. [[CrossRef](#)]
31. Mishra, R.K.; Kumar, V.; Mohanty, K. Pyrolysis kinetics behaviour and thermal pyrolysis of *Samanea saman* seeds towards the production of renewable fuel. *J. Energy Inst.* **2020**, *93*, 1148–1162. [[CrossRef](#)]
32. Aboulkas, A.; Hammani, H.; El Achaby, M.; Bilal, E.; Barakat, A. Valorization of algal waste via pyrolysis in a fixed-bed reactor: Production and characterization of bio-oil and bio-char. *Bioresour. Technol.* **2017**, *1*, 400–408. [[CrossRef](#)] [[PubMed](#)]
33. Sayed, A.S.; Abdelmottaleb, M.; Cheira, M.F.; Abdel-Aziz, G.; Gomaa, H.; Hassanein, T.F. Date seed as an efficient, eco-friendly, and cost-effective bio-adsorbent for removal of thorium ions from acidic solutions. *Aswan Univ. J. Environ. Stud.* **2020**, *1*, 106–124. [[CrossRef](#)]
34. Al Haddabi, M.; Ahmed, M.; Al Jebri, Z.; Vuthaluru, H.; Znad, H.; Al Kindi, M. Boron removal from seawater using date palm (*Phoenix dactylifera*) seed ash. *Desalination Water Treat.* **2016**, *57*, 5130–5137. [[CrossRef](#)]
35. Mahdi, Z.; El Hanandeh, A.; Yu, Q.J. Preparation, characterization and application of surface modified biochar from date seed for improved lead, copper, and nickel removal from aqueous solutions. *J. Environ. Chem. Eng.* **2019**, *7*, 103379. [[CrossRef](#)]
36. Khiari, B.; Jeguirim, M. Pyrolysis of Grape Marc from Tunisian Wine Industry: Feedstock Characterization, Thermal Degradation and Kinetic Analysis. *Energies* **2018**, *11*, 730. [[CrossRef](#)]
37. Ondro, T.; Vitázek, I.; Húlan, T.; Lawson, M.K.; Csáki, Š. Non-isothermal kinetic analysis of the thermal decomposition of spruce wood in air atmosphere. *Res. Agric. Eng.* **2018**, *64*, 41–46.
38. Gao, W.; Chen, K.; Zeng, J.; Xu, J.; Wang, B. Thermal pyrolysis characteristics of macroalgae *Cladophora glomerata*. *Bioresour. Technol.* **2017**, *243*, 212–217. [[CrossRef](#)]
39. Yao, Z.; Yu, S.; Su, W.; Wu, W.; Tang, J.; Qi, W. Kinetic studies on the pyrolysis of plastic waste using a combination of model-fitting and model-free methods. *Waste Manag. Res.* **2020**, *38*, 77–85. [[CrossRef](#)]
40. Yao, Z.; Yu, S.; Su, W.; Wu, W.; Tang, J.; Qi, W. Comparative study on the pyrolysis kinetics of polyurethane foam from waste refrigerators. *Waste Manag. Res.* **2020**, *38*, 271–278. [[CrossRef](#)]